

# Ab initio and DFT calculations of 2-Amino-1(4-Bromo-phenyl)-5-oxo-4, 5-dihydro-1-H-pyrrole-3-carboxylic acid ethyl ester

<sup>1</sup>Patel B. D. \*, <sup>2</sup>Patel U. H. and <sup>3</sup>Shah D. A.

<sup>1</sup>Natubhai V. Patel College of Pure and Applied Sciences, Vallabh Vidyanagar 388120, Gujarat, India

<sup>2</sup>Department of Physics, Sardar Patel University, Vallabh Vidyanagar 388120, Gujarat, India

<sup>3</sup>Organic Synthesis Laboratory, M. G. Science Institute, Ahmedabad, Gujarat, India

DOI: 10.6088/ijaser.020300019

**Abstract:** The molecular structure of 2-Amino-1(4-Bromo-phenyl)-5-oxo-4, 5-dihydro-1-H-pyrrole-3-carboxylic acid ethyl ester, has crystallographic parameters  $a = 15.1482(59)$ ,  $b = 7.7385(32)$ ,  $c = 12.6585(50)$  Å and  $\beta = 114.697(0)^\circ$ , crystallized in to monoclinic crystal system with space group  $P2_1/c$ . To determine total energy, molecular energies and atomic charge distributions and also to calculate bond lengths, bond angles and torsional angles of the title compound, ab initio and DFT calculations have been carried out by Gaussian-09 software performed at HF and B3LYP methods using the same basis set 6-311G\*. The computed geometrical parameters are in good agreement with the experimental results.

**Key words:** Molecular structure; Crystal system; Total energy; Atomic charge distribution.

## 1. Introduction

Pyrrole, belonging to an important heterocyclic compounds, possesses a variety of biological activity such as anticancer, aldose reductase inhibition, anti-inflammatory and analgesic activities (Burnham *et al.*, 1998; Fan *et al.*, 2008; Mayer *et al.*, 2009; Manzanaro *et al.*, 2006). In polymerization process, pyrroles and its derivatives are widely used as corrosion inhibitors, preservatives, and as solvents for resins and terpenes and are also used in metallurgical processes (Bonnet, R. 1995; Grive, M. B. et al., 1994). The title compound, 2-Amino-1(4-Bromo-phenyl) -5-oxo-4, 5-dihydro-1-H-pyrrole-3-carboxylic acid ethyl ester,  $C_{13}H_{13}BrN_2O_3$ , is one of the series of substituted pyrrole derivatives which are being synthesized, investigated and reported by us, as a part of studying systematically the heterocyclic compounds (Patel *et al.*, 2001; Patel *et al.*, 2007). To compare the experimental results with the theoretical methods, for the title compound using different molecular geometries, the ab-initio and DFT calculations are carried out to determine bond lengths, bond angles and torsional angles of molecule by calculating the total energy of a molecule. The dipole moment and molecular energies like HOMO (Highest occupied molecular orbital) and LUMO (Lowest Unoccupied Molecular Orbital) are also calculated. Both the ab-initio and the density functional theory (DFT) methods have become an increasingly useful tool for theoretical studies. The success of the study of these methods is mainly due to the fact that it describes the small molecules more reliably and therefore in this paper, an intensive approach by X- ray crystallography and quantum calculations is used, which takes advantage of both the high interpretive power of the theoretical studies and the precision and reliability of the experimental method (Patel *et al.*, 2012).

## 2. Experimental

The synthesis and crystal structure of the title compound has been earlier reported by us (Patel *et al.*, 2012). The ORTEP diagram of the title molecule showing 50% probability displacement ellipsoids with

\*Corresponding author (e-mail: fbdpatel@gmail.com)

Received on May 2013; Accepted on May 2013; Published on June 2013

numbering scheme is shown in Figure: 1.

### 3. Computational methods

Using Gaussian-09 program package, the quantum chemical calculations using ab-initio and density functional theory (DFT) methods at the HF/ 6-311G\* and B3LYP/ 6-311G\* levels were performed for the title compound (Frisch et al, 2009). All the theoretical calculations using the default convergences criteria were carried out at Department of Physics, Sardar Patel University, Vallabh Vidyanagar.

## 4. Results and Discussion

### 4.1 Molecular geometry

Using Gaussian-09 programme, the ab initio and density functional theory (DFT) calculations at the HF/ 6-311G\* and B3LYP/ 6-311G\* levels of the theory were performed for the title compound. From the calculations, selected optimized geometric parameters bond lengths, bond angles and torsional angles are listed in Table: 1, Table: 2 and Table: 3 respectively and compared with those of the experimental values. In view of the bond lengths in Table: 1, the biggest difference between theoretical and experimental values occurs at C13-C12 bond with the difference 0.0449 Å for B3LYP method and at O1-C7 bond, with the different values being 0.0429 Å for HF method. In bond angles, most predicted values are corresponding to the experimental values and the biggest difference takes place at the bond angle of N1-C7-C8, with difference value of 2.3748° and at the bond angle of O2-C12-C13, with difference value of 2.011° for B3LYP and HF methods respectively. The differences between the calculated and observed geometry could be related to the crystal packing in the molecules. However, the inspection of collective intermolecular interactions C-H...O, N-H...O,  $\pi$ - $\pi$  and C-O... $\pi$  provides evidence of collective effect of all these interactions on crystal packing in the unit cell.

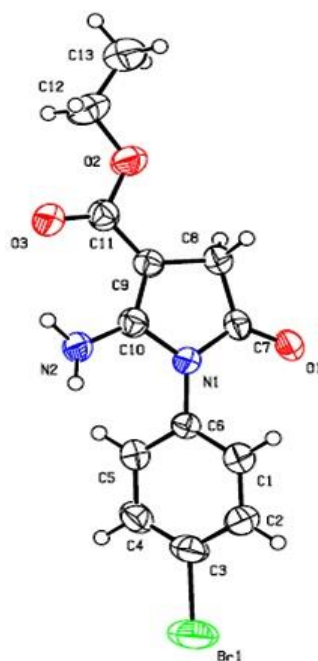


**Figure 1:** The ORTEP diagram of the title molecule showing 50% probability displacement ellipsoids

**Table 1:** Comparison of bond lengths obtained by HF and B3LYP methods with experimental values

Sr. No.	Atoms	Bond lengths (Å) calculation using		
		Exp.	B3LYP/ 6-311G*	HF/ 6-311G*
1.	C1-C2	1.378(7)	1.3907	1.3829
2.	C2-C3	1.388(7)	1.3919	1.3828
3.	C3-C4	1.353(7)	1.391	1.3818
4.	C4-C5	1.381(7)	1.3922	1.3843
5.	C5-C6	1.366(5)	1.3987	1.3851
6.	C6-C1	1.389(7)	1.3975	1.3849
7.	C7-C8	1.491(7)	1.5232	1.5153
8.	C8-C9	1.492(6)	1.5015	1.5028
9.	C9-C10	1.362(7)	1.372	1.3576
10.	C9-C11	1.418(7)	1.4353	1.4382
11.	C13-C12	1.470(9)	1.5149	1.5121
12.	N1-C6	1.432(6)	1.4232	1.4228
13.	N1-C7	1.380(5)	1.4194	1.3979
14.	N1-C10	1.416(6)	1.4025	1.3885
15.	N2-C10	1.344(6)	1.3516	1.3405
16.	O1-C7	1.224(5)	1.2038	1.1811
17.	O2-C11	1.357(6)	1.357	1.3256
18.	O2-C12	1.416(7)	1.4431	1.4208
19.	O3-C11	1.208(6)	1.2281	1.2013
20.	Br1-C3	1.896(5)	1.9152	1.8979

**Table 2:** Comparison of bond angles obtained by B3LYP and HF methods with experimental values

Sr. No.	Atoms	Bond angles (°) calculation using		
		Exp.	B3LYP/ 6-311G*	HF/ 6-311G*
1.	C6-C1-C2	120.1(4)	120.2062	120.214
2.	C1-C2-C3	118.4(4)	119.5307	119.3744
3.	C4-C3-C2	121.7(5)	120.9399	120.9809
4.	Br1-C3-C2	118.7(4)	119.5418	119.5122
5.	Br1-C3-C4	119.6(4)	119.5177	119.5067
6.	C5-C4-C3	119.7(4)	119.3556	119.2846
7.	C6-C5-C4	120.0(4)	120.2977	120.2571
8.	C5-C6-C1	120.1(4)	119.6504	119.8789
9.	N1-C6-C1	118.8(3)	119.8464	119.9073
10.	N1-C6-C5	121.1(4)	120.4849	120.2094
11.	O1-C7-C8	127.2(3)	128.872	128.6506
12.	O1-C7-N1	123.8(4)	124.5024	124.2881
13.	N1-C7-C8	109.0(3)	106.6252	107.0612

14. C9-C8-C7	102.9(3)	103.6414	102.7992
15. C8-C9-C10	108.8(4)	108.8104	108.8986
16. C8-C9-C11	128.8(4)	128.9715	128.3382
17. C10-C9-C11	122.4(4)	122.0953	122.733
18. C9-C10-N1	110.4(4)	110.9606	110.9314
19. C9-C10-N2	129.9(5)	127.7419	129.0284
20. N1-C10-N2	119.8(4)	121.2862	120.0208
21. O2-C11-O3	122.2(4)	122.3341	122.4359
22. C9-C11-O2	111.0(4)	112.5272	112.6952
23. C9-C11-O3	126.7(5)	125.1379	124.8684
24. O2-C12-C13	109.5(5)	107.389	107.489
25. C6-N1-C10	126.8(3)	126.1913	126.0223
26. C7-N1-C6	123.5(3)	123.8543	123.6576
27. C7-N1-C10	108.8(4)	109.9253	110.2956
28. C11-O2-C12	117.3(4)	116.3105	117.8347

**Table 3:** Comparison of torsional angles obtained by RHF and B3LYP methods with experimental values

Sr. No.	Atoms	Torsional angles (°)		
		Exp.	B3LYP/ 6-311G*	HF/ 6-311G*
1.	C6-C1-C2-C3	-2.0(7)	0.5923	0.5756
2.	C1-C2-C3-C4	0.3(7)	-0.8768	-0.6175
3.	C1-C2-C3-Br1	179.5(3)	179.4153	179.5332
4.	C5-C4-C3-C2	1.3(7)	-0.0437	-0.1531
5.	C5-C4-C3-Br1	-177.9(3)	179.6643	179.6962
6.	C4-C5-C6-C1	-0.6(6)	-1.5284	-1.0127
7.	C4-C5-C6-N1	177.1(4)	-179.9684	179.7539
8.	C5-C6-C1-C2	2.2(6)	0.5986	0.2322
9.	N1-C6-C1-C2	-175.5(4)	179.0486	179.4679
10.	N1-C7-C8-C9	-4.6(4)	-1.8704	-1.1738
11.	O1-C7-C8-C9	175.9(4)	178.343	178.7685
12.	C10-C9-C8-C7	4.3(4)	1.2792	0.9613
13.	C11-C9-C8-C7	-177.2(4)	-174.696	-177.0614
14.	C11-C9-C10-N1	178.9(4)	176.1042	177.7545
15.	C11-C9-C10-N2	-0.9(7)	-5.1217	-3.876
16.	C8-C9-C11-O2	5.7(6)	-2.1424	-1.2843
17.	C8-C9-C11-O3	-176.5(4)	-177.5414	-178.4617
18.	C10-C9-C11-O2	-176.1(4)	-177.6443	-179.0603
19.	C10-C9-C11-O3	1.7(7)	2.0395	0.6857
20.	C7-N1-C6-C5	-122.0(4)	128.3746	113.5749
21.	C7-N1-C6-C1	55.7(5)	-50.0623	-65.6583
22.	C10-N1-C6-C5	45.3(6)	-49.463	-64.4424

23.	C10-N1-C6-C1	-137.1(4)	132.1	116.3244
24.	C6-N1- C7- O1	-8.0(6)	3.5093	2.78
25.	C6-N1- C7-C8	172.5(3)	176.2891	177.2745
26.	C10-N1- C7-O1	-177.2(4)	-178.3469	-178.9296
27.	C10-N1- C7-C8	3.3(4)	1.8548	1.0159
28.	C6-N1-C10-C9	-169.2(4)	177.011	177.837
29.	C7-N1-C10-C9	-0.5(4)	-1.079	-0.4036
30.	C7-N1-C10-N2	179.3(4)	-179.9446	-178.9407
31.	C6-N1-C10-N2	10.6(6)	-1.8546	-0.7002

In addition to this, we also studied the relation between the experimental and calculated results by comparing them and obtaining the linear function formulae of  $y = 1.041x - 0.056$  ( $R^2 = 0.980$ ) for HF/6-311G\*\* and  $y = 1.025x - 0.021$  ( $R^2 = 0.984$ ) for B3LYP/6-311G\*\* for bond lengths and  $y = 0.986x + 1.619$  ( $R^2 = 0.980$ ) for HF/6-311G\*\* and  $y = 0.984x + 1.779$  ( $R^2 = 0.974$ ) for B3LYP/6-311G\*\* bond angles as shown in Figure: 2.

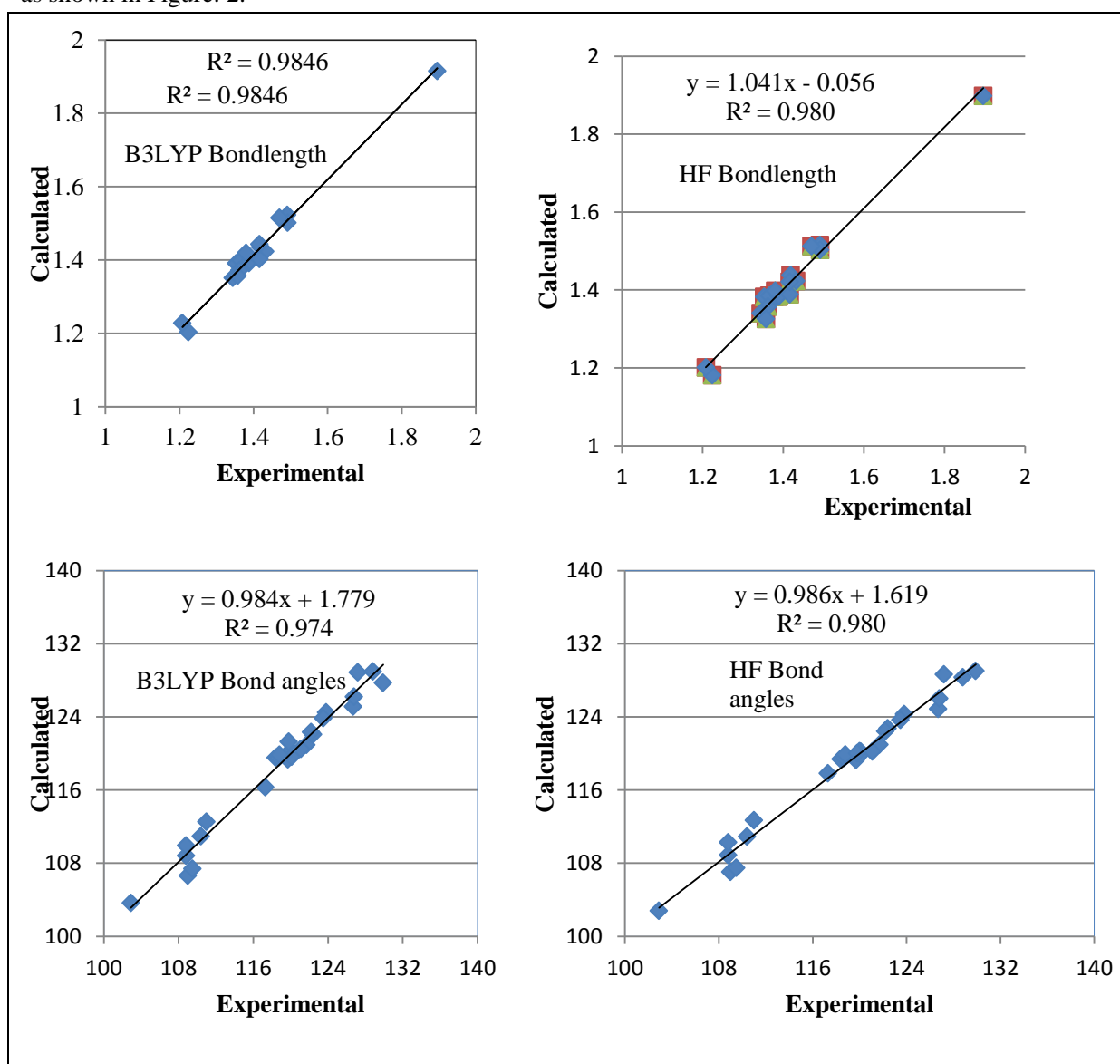


**Figure 2:** Computational correlation of bond lengths and bond angles for B3LYP and HF methods

## 4.2 HOMO and LUMO analysis

The wave function analysis indicates that the electron absorption corresponds to the transition from the ground state to the first excited state and is mainly described by one electron excitation from the highest occupied molecular orbital (HOMO) to the lowest unoccupied molecular orbital (LUMO). The HOMO-LUMO energy gap calculated for the title compound is -0.17141 and -0.40897 at the B3LYP/6-311G\* and HF/6-311G\* methods respectively. The chemical activity of the molecule is reflected by the energy gap. In Table: 4, HOMO and LUMO energy calculations, Total energy (a.u.) and Dipole moment (D) of the title compound using both the methods are listed.

**Table 4:** HOMO and LUMO energy calculation, Total energy (a.u.) and Dipole moment (D) for the title compound using different methods

Methods	HOMO	LUMO	$\Delta E$	Total energy (a.u.)	Dipole moment (D)
B3LYP/6-311G*	-0.21650	-0.04509	-0.17141	-3412.5603	1.9571
HF/6-311G*	-0.31232	0.09665	-0.40897	-3405.7376	2.1066

## 4.3 Mulliken population analysis

The Mulliken population analysis of the title molecule has been calculated using HF/6-311G\* and B3LYP/6-311G\* methods and shown in Table: 5. The chart of Mulliken charge distribution is shown in Figure: 3. It is observed that the nitrogen atom N2 has negative charge (-0.857661 and -1.015841), the carbon atom C13 has negative charge (-0.625488 and -0.630104), the carbon atom C8 has negative charge (-0.541284 and -0.551246), the nitrogen N1 has negative charge (-0.515057 and -0.678393), the oxygen atom O3 has negative charge (-0.432908 and -0.555355), the oxygen atom O2 has negative charge (-0.337097 and -0.452502), the oxygen atom O1 has negative charge (-0.324234 and -0.441994), and the carbon atom C10 has highest positive charge (0.666085 and 0.871355) using B3LYP and HF methods respectively. Among all non-hydrogen atoms, the nitrogen atoms N2, N1 and carbon atom C13 have more negative charge and carbon atoms C10 and C11 have more positive charges. Nitrogen atoms N1 and N2 are connected with highest opposite positive charged carbon atom C10. Similarly all the hydrogen atoms have a net positive charge in particular; the hydrogen atoms H90 and H91 have significantly large net positive charges. The presence of considerable amount of charges on N1, N2, O1, O2, O3 and the hydrogens H90 and H91 atoms predict the presence of intermolecular hydrogen bondings in the crystalline phase, which has been confirmed from the crystallographic investigations.

**Table 5:** Calculation of Mulliken charge for the title compound using B3LYP/6-311G\* and HF/6-311G\* level.

Sr. no.	Atom	Mulliken charge using	
		B3LYP	HF
1.	C1	-0.165006	-0.174760
2.	C2	-0.165685	-0.171811
3.	C3	-0.117538	-0.139467

4.	C4	-0.157676	-0.165433
5.	C5	-0.217469	-0.208639
6.	C6	0.168669	0.188176
7.	C7	0.435459	0.618856
8.	C8	-0.541284	-0.551246
9.	C9	-0.253615	-0.395249
10.	C10	0.666085	0.871355
11.	C11	0.462368	0.685597
12.	C12	-0.211050	-0.153435
13.	C13	-0.625488	-0.630104
14.	N1	-0.515057	-0.678393
15.	N2	-0.857661	-1.015841
16.	O1	-0.324234	-0.441994
17.	O2	-0.337097	-0.452502
18.	O3	-0.432908	-0.555355
19.	Br1	-0.019535	-0.029353
20.	H1	0.227975	0.244131
21.	H2	0.225471	0.254611
22.	H4	0.224484	0.254349
23.	H5	0.232373	0.247906
24.	H8a	0.249930	0.258756
25.	H8b	0.251912	0.259887
26.	H90	0.384859	0.430907
27.	H91	0.353534	0.385361
28.	H12a	0.211296	0.212365
29.	H12b	0.210360	0.211111
30.	H13a	0.214095	0.215431
31.	H13b	0.209061	0.209888
32.	H13c	0.213370	0.214896

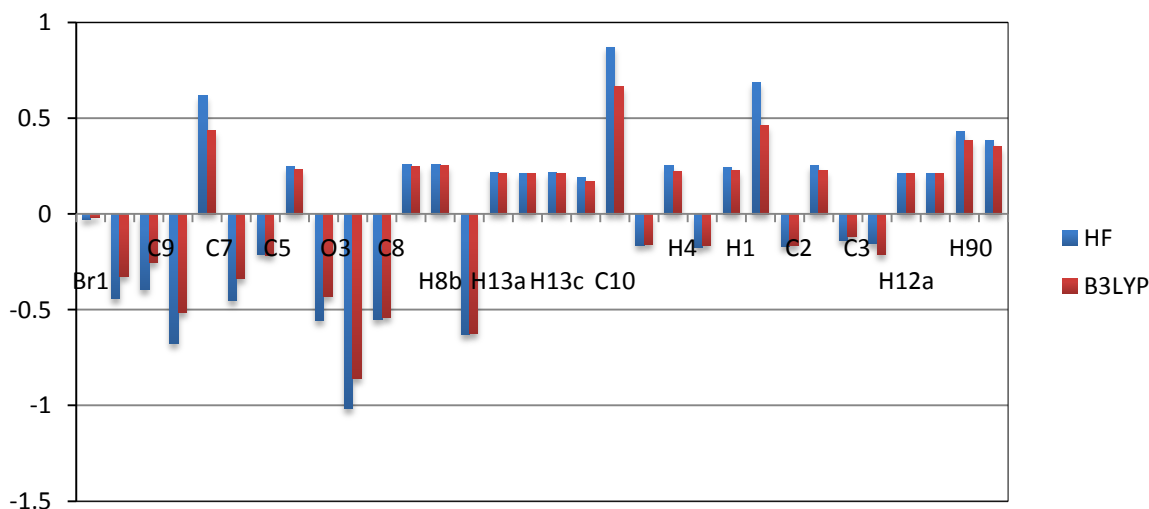


**Figure 3:** Mulliken charge distribution charts of the title compound using B3LYP/ 6-311G\* shown as Series 1 and HF/ 6-311G\* level Shown as Series 2.

## 5. Conclusions

The optimized geometries and HOMO-LUMO analysis of 2-Amino-1(4-Bromo-phenyl)-5-oxo-4,5-dihydro-1-H-pyrrole-3-carboxylic acid ethyl ester were performed and analyzed at HF and DFT methods like B3LYP level of theories utilizing 6-311G\* (d) and 6-311G\* basis sets. The data obtained during the course of present investigation show that a better conformity between the experimental and computed data is obtained by the DFT method of B3LYP level with a 6-311G\* basis set. From the study of Mulliken population analysis, it has been observed that the presence of high negative charge and high positive charge of atoms predicts more chance of chemical bonding among those atoms in the molecule. The least negative charge observed for Br atom reveals the facts that it is not involved in any kind of intra or inter molecular interactions in the molecular packing of the structure.

## Acknowledgement

The authors are grateful to Department of Physics, Sardar Patel University, Vallabh Vidyanagar for providing the computer facility to carry out the research work. BDP is also thankful to Natubhai V Patel College of Pure and Applied Sciences, Vallabh Vidyanagar for giving the necessary permission to carry out the research work and UGC for funding towards the minor research project (No. 47-2163/11 (WRO)).

## 6. References

1. Burnham, B. S., Gupton, J. T., Krumpe, K., Webb, T., Shuford, J., Bowers, B., Warren, A. E., Barnes, C. & Hall, I. H. (1998). Cytotoxicity of substituted alkyl-3,4-bis(4-methoxyphenyl) pyrrole-2-carboxylates in L1210 lymphoid leukemia cells. *Arch.Pharm. Pharm. Med. Chem.* 331, 337–341.
2. Fan, H., Peng, J., Hamann, M. T. & Hu, J. F. (2008). Lamellarins and Related Pyrrole-Derived Alkaloids from Marine Organisms. *Chem. Rev.* 108, 264-287.
3. Mayer A. M., Rodríguez A. D., Berlinck R. G. and Hamann M.T., 2009. Marine pharmacology in 2005-6: Marine compounds with anthelmintic, antibacterial, anticoagulant, antifungal, anti-inflammatory, antimalarial, antiprotozoal, antituberculosis, and antiviral activities; affecting the cardiovascular, immune and nervous systems, and other miscellaneous mechanisms of action. *Biochim Biophys Acta.*, 1790 (5):283-308. DOI:10.1016/j.bbagen.2009.03.011.
4. Manzanaro, S., Salva, J., and de la Fuente, J. A. 2006. Phenolic marine natural products as aldose reductase inhibitors. *J. Nat. Prod.*, 69, 1485-1487.
5. Bonnet, R. 1995. Photosensitizers of the porphyrin and phthalocyanine series for photodynamic therapy. *Chem. Soc. Rev.*, 24, 19-33.
6. Grive, M. B., Hudson, A. J., Richardson, Johnstone, R. A. W., Sorbal, A. J. F. N. and Rocha Gonsalves, A. M. d'. 1994. An investigation of the optical properties of tetraphenylporphyrin derivatives in Langmuir and Langmuir-Blodgett films, *Thin solid films*, 243(1-2), 581-586.



7. Patel, U. H., Patel, B. H. and Patel, B. N; 2001. Crystal and Molecular Structure of Sulfadimethoxine, Polymorph III, *Crystal Research and Technology*, 36, 1445-1450.
8. Patel, U. H., Patel, B. D., Modh, R. D. and Patel, P. D. 2007. 1,1'-Sulfonyldiimidazole, *Acta Crystallographica*, E63, o3598-o3599. DOI:10.1107/S160053680703543X.
9. Patel, U. H. and Patel, B. D. 2012. Quantum chemical studies on crystal structure of 1, 1' sulfonyldiimidazole. *Int. Journal of Applied Sciences and Engineering Research*, Vol. 1(4), 7595-603. DOI:10.6088/ijaser.0020101061.
10. Patel B. D., Patel U. H. and Shah D. A. 2012. Synthesis and crystal structure determination of 2-Amino-1 (4-Bromo-phenyl)-5-oxo-4, 5-dihydro-1-H-pyrrole-3-carboxylic acid ethyl ester. *Int. Journal of Applied Sciences and Engineering Research*, Vol. 1(6), 755-762. DOI:10.6088/ijaser.0020101076.
11. Gaussian 09, 2009. Revision A.1, Frisch, M. J.; Trucks, G. W.; Schlegel, H. B.; Scuseria, G. E.; Robb, M. A.; Cheeseman, J. R.; Scalmani, G.; Barone, V.; Mennucci, B.; Petersson, G. A.; Nakatsuji, H.; Caricato, M.; Li, X.; Hratchian, H. P.; Izmaylov, A. F.; Bloino, J.; Zheng, G.; Sonnenberg, J. L.; Hada, M.; Ehara, M.; Toyota, K.; Fukuda, R.; Hasegawa, J.; Ishida, M.; Nakajima, T.; Honda, Y.; Kitao, O.; Nakai, H.; Vreven, T.; Montgomery, Jr., J. A.; Peralta, J. E.; Ogliaro, F.; Bearpark, M.; Heyd, J. J.; Brothers, E.; Kudin, K. N.; Staroverov, V. N.; Kobayashi, R.; Normand, J.; Raghavachari, K.; Rendell, A.; Burant, J. C.; Iyengar, S. S.; Tomasi, J.; Cossi, M.; Rega, N.; Millam, J. M.; Klene, M.; Knox, J. E.; Cross, J. B.; Bakken, V.; Adamo, C.; Jaramillo, J.; Gomperts, R.; Stratmann, R. E.; Yazyev, O.; Austin, A. J.; Cammi, R.; Pomelli, C.; Ochterski, J. W.; Martin, R. L.; Morokuma, K.; Zakrzewski, V. G.; Voth, G. A.; Salvador, P.; Dannenberg, J. J.; Dapprich, S.; Daniels, A. D.; Farkas, Ö.; Foresman, J. B.; Ortiz, J. V.; Cioslowski, J.; Fox, D. J. Gaussian, Inc., Wallingford CT.